Available online at www.sciencedirect.com
ScienceDirect
Journal of the European Ceramic Society 29 (2009) 551–557
www.elsevier.com/locate/jeurceramsoc

Thermal properties of single-phase Y_2SiO_5

Ziqi Sun [a,b], Meishuan Li [a], Yanchun Zhou [a,*]

[a] *Shenyang National Laboratory for Materials Science, Institute of Metal Research, Chinese Academy of Sciences, Shenyang 110016, China*
[b] *Graduate School of Chinese Academy of Sciences, Beijing 100039, China*

Received 9 May 2008; received in revised form 19 June 2008; accepted 4 July 2008
Available online 28 August 2008

Abstract

Y_2SiO_5 is a promising candidate for oxidation-resistant or environmental/thermal barrier coatings (ETBC) due to its excellent high-temperature stability, low elastic modulus and low oxygen permeability. In this paper, we investigated the thermal properties of Y_2SiO_5 comprehensively, including thermal expansion, thermal diffusivity, heat capacity and thermal conductivity. It is interesting that Y_2SiO_5 has a very low thermal conductivity (~1.40 W/m K) but a relatively high linear thermal expansion coefficient ($(8.36 \pm 0.5) \times 10^{-6}\,K^{-1}$), suggesting compatible thermal and mechanical properties to some non-oxide ceramics and nickel superalloys as ETBC layer. Y_2SiO_5 is also an ideal EBC on YSZ TBC layer due to their close thermal expansion coefficients. As a continuous source of Y^{3+}, it is predicted that Y_2SiO_5 EBC may prolong the lifetime of zirconia-based TBC by stopping the degradation aroused by the loss of Y stabilizer.

Keywords: Y_2SiO_5; Thermal properties; Silicate; Thermal conductivity; Engine components

1. Introduction

Si-based ceramics, such as silicon carbide and silicon nitride, have superior high-temperature strength and creep resistance, and show potential to improve gas turbine engine performance. However, the lack of environmental durability in combustion environments impedes the applications of these materials.[1–3] Therefore, a protective coating is in need. Recently, experimental trials have proven that $Y_2Si_2O_7$, Y_2SiO_5 as well as $Lu_2Si_2O_7$, $Yb_2Si_2O_7$ are promising candidates for environmental barrier coatings (EBC) on silicon-based ceramics.[4–6]

Yttrium silicate (Y_2SiO_5) is an important laser crystal that has been synthesized by a chemical method since 1963.[7] Most research activities are related to rare earth (Ce^{3+}, Eu^{3+}, etc.) doped Y_2SiO_5 crystals to be used as blue phosphor or Cr^{4+}-doped Y_2SiO_5 as a saturable-absorber Q-switch laser.[8–10] As an important phase in the SiO_2–Y_2O_3–Si_3N_4 phase diagram,[11,12] Y_2SiO_5 is frequently identified as a precipitated phase at the grain boundaries of sintered Si_3N_4 with Y_2O_3 or $Y_2O_3 + SiO_2$ as sintering aids. And it is confirmed that Y_2SiO_5 can improve the high-temperature performance of silicon nitride.[12–14] The melting point of Y_2SiO_5 is up to 1950 °C guaranteeing its potential high-temperature structural applications.[15] Although the spectroscopic studies of doped Y_2SiO_5 have been widely performed, the fundamental properties of the host crystal itself are still in dearth.

Recently, Y_2SiO_5 has attracted wide attentions and a number of published works have focused on its coating applications,[20–24] which were aroused by two interesting characteristics of Y_2SiO_5. Firstly, Y_2SiO_5 has a low oxygen permeability over a wide temperature range, as reported by Ogura et al., the oxygen permeability constant is 10^{-10} kg/(m s) at 1973 K.[16] Secondly, the thermal expansion coefficient of Y_2SiO_5 (Table 1) matches well with some non-oxide materials such as silicon-based ceramics, C/C composites and so on, especially in combination with $Y_2Si_2O_7$.[17–22]

However, the preparation of single-phase and fully dense Y_2SiO_5 bulk material is very difficult. The synthesis of Y_2SiO_5 is always accompanied with the presence of undesired compounds such as $Y_{4.67}(SiO_4)_3O$, $Y_2Si_2O_7$, etc., as well as incomplete polymorph transformation between the low-temperature phase (X1-Y_2SiO_5) and high-temperature phase (X2-Y_2SiO_5). Impurities have a strong influence on the final properties of Y_2SiO_5. For example, the measured thermal

* Corresponding author at: High-performance Ceramic Division, Shenyang National Laboratory for Materials Science, Institute of Metal Research, Chinese Academy of Sciences, 72 Wenhua Road, Shenyang 110016, China.
Tel.: +86 24 23971765; fax: +86 24 23891320.
E-mail address: yczhou@imr.ac.cn (Y. Zhou).

0955-2219/$ – see front matter © 2008 Elsevier Ltd. All rights reserved.
doi:10.1016/j.jeurceramsoc.2008.07.026

Table 1
Reported thermal expansion coefficients for Y_2SiO_5

Material	Temperature (K)	TEC ($\times 10^{-6}$ K^{-1})	Reference
Single crystal Y_2SiO_5	300–1000	$\alpha_a = 0.6$ $\alpha_b = 7.5$ $\alpha_c = 11.4$ $\frac{\Delta V}{V \Delta T} = 17$	O'Bryan et al.[17]
Y_2SiO_5 powders	293–1123	$\alpha_a = 5.2$ $\alpha_b = 7.5$ $\alpha_c = 10.7$	Nowok et al.[18]
	1123–1673	$\alpha_a = 19.5$ $\alpha_b = 12.5$ $\alpha_c = 25$	
X1-Y_2SiO_5 powders	394–1273	$\alpha = 5.0 \times 0.00421T$	Fukuda and Matsubara[19]
X2-Y_2SiO_5 powders	394–1473	$\alpha = 5.0 \times 0.00257T$	
Polycrystalline bulk material ($Y_2SiO_5 + Y_{4.67}(SiO_4)_3O$)	300–1623	$\alpha = 5.3$	Ogura et al.[20]
Polycrystalline bulk material ($Y_2SiO_5 + Y_2O_3$)	300–1273	$\alpha = 6.9$	Apricio and Duran[21]
Polycrystalline bulk material	300–1173	$\alpha = 3.05$	Wagner et al.[22]
	1173–1673	$\alpha = 4.09$	
Single-phase polycrystalline Y_2SiO_5 bulk material	300–1573	$\alpha = 8.36$	Present work

expansion coefficients of Y_2SiO_5 in Table 1 show a wide deviation from author to author, which was mainly caused by the undesired impurities. The fundamental properties such as mechanical and thermal properties for single-phase Y_2SiO_5 are seldom investigated. But these data are indispensable for selection of Y_2SiO_5 as candidate for both high-temperature structural components and coatings.

In our previous paper, we successfully synthesized single-phase Y_2SiO_5 powders (X2-Y_2SiO_5, here after written as Y_2SiO_5 for brevity) from Y_2O_3 and SiO_2 powders,[25] and evaluated its mechanical properties.[26] Y_2SiO_5 has low Young's modulus but high damage tolerance, which endow the promising coating applications of Y_2SiO_5 from the view of mechanical properties. In this paper, the thermal expansion coefficient of polycrystalline Y_2SiO_5 was investigated by measuring the dimension variation of cylindrical specimens using push-rod thermal expansion dilatometer. Other thermal properties, e.g. thermal diffusivity, thermal capacity and thermal conductivity were also studied. These thermal property data are helpful for the further design of Y_2SiO_5 as coatings or high-temperature structural components.

2. Experimental procedure

Y_2SiO_5 powders were synthesized via a solid/liquid reaction method. The initial yttria and silica powders were calcined with 3 mol.% $LiYO_2$ additive at 1500 °C for 2 h in air. Bulk material with 98% theoretical density was obtained by pressureless sintering of the synthesized Y_2SiO_5 powders at 1500 °C for 60 min in air. Details of the preparation can be found in our previous work.[25] Fig. 1(a) presents the microstructure of the thermal etched surface of Y_2SiO_5 material via heating to 1300 °C with a rate of 10 °C/min, holding for 30 min, and then cooling to room temperature with a rate of 15–20 °C/min. The sample displays equiaxed grains in the majority with an average grain size of

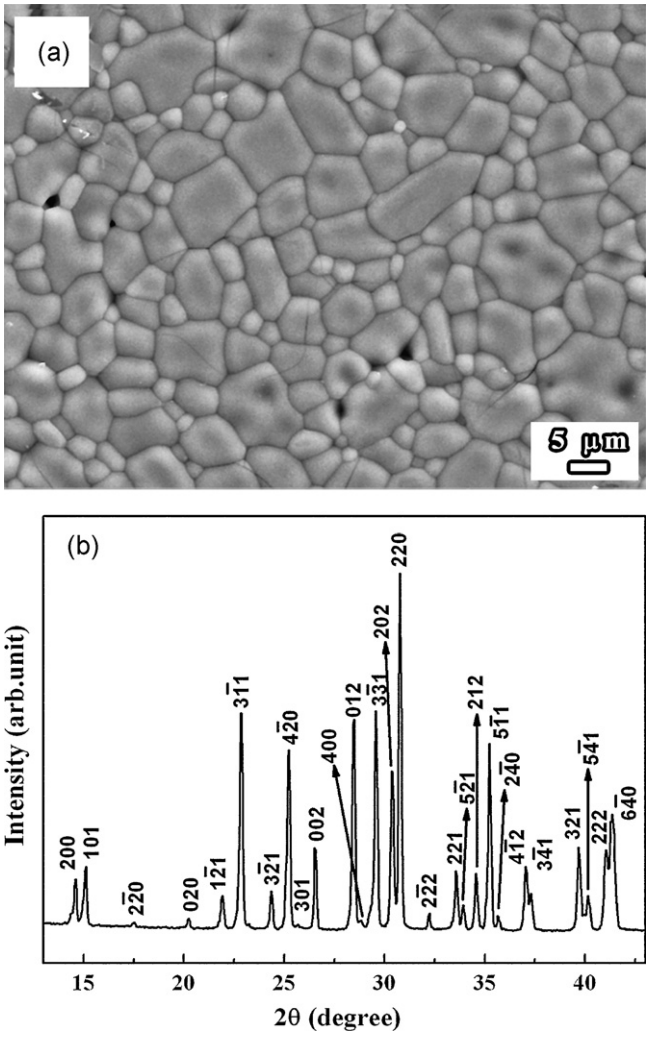

Fig. 1. (a) Microstructure of the thermal etched surface of Y_2SiO_5, and (b) XRD pattern collected on the sintered material.

about 6 μm. A few residual small pores can be found in the sintered material, and all the pores exist at the grain boundaries. Fig. 1(b) shows a XRD pattern collected on the sample after sintering. It is clear that the sintered material is single-phase Y_2SiO_5 and without visible preferred orientation.

The average linear thermal expansion coefficient was obtained from the temperature dependent changes of the length of the specimen from room temperature to 1573 K in air by using a high-temperature dilatometer (Setaram Setsys 24, Caluire, France). The data were continuously recorded during heating at a rate of 2 K/min as well as cooling processes. The specimens were cylindrical pieces with 6 mm in diameter and 8 mm in height.

The thermal diffusivity measurement was conducted on a Flashline 5000 thermal properties analyzer (Anter Corporation, Pittsburg, USA) according to the procedure described in ASTM E1461-01, which is based on delivering a pulse of thermal energy to one face of the analyzed sample and monitoring the temperature rise of the opposite face.[27] The thermal diffusivity, D_{th} (cm^2/s) is evaluated from sample thickness L (cm), and the time, $t_{1/2}$ (s), elapsed from the moment when the pulse of thermal energy is delivered to the moment when the temperature of the opposite face of the sample reaches half of its maximum:

$$D_{th} = \frac{0.13879L^2}{t_{1/2}} \quad (1)$$

To measure the constant pressure molar heat capacity C_p and thermal conductivity κ, a disc sample (Ø 12.7 mm × 1.0 mm) was used. The thermal conductivity was determined in the temperature range from 473 to 1273 K. Prior to the thermal diffusion test the samples was sprayed with a thin layer of colloidal graphite to ensure complete and uniform absorption of the laser pulse. Three measurements were taken at each temperature and the data were recorded using an Anter FL5000 software. Employing a multi-sample configuration system and testing a reference sample (graphite) adjacent to Y_2SiO_5, the heat capacity of Y_2SiO_5 can be obtained in parallel with thermal diffusivity.[28] Then, the thermal diffusivity results were converted to thermal conductivities using the heat capacity results and measured density of Y_2SiO_5. Thermal conductivity was calculated from the values of thermal diffusivity, specific heat capacity, and measured density, according to the relation:

$$\kappa(T) = D_{th}(T)C_p(T)\rho(T) \quad (2)$$

3. Results and discussions

3.1. Thermal properties of Y_2SiO_5

Thermal expansion of polycrystalline Y_2SiO_5 measured by the push-rod dilatometer was illustrated in Fig. 2. With the increasing of temperature to 1573 K, the length of Y_2SiO_5 samples expanded linearly. Since the as-sintered sample has no preferable orientation (Fig. 1(b)), an isotropic thermal expansion for Y_2SiO_5 bulk materials was observed. The fractional change in the linear thermal expansion of Y_2SiO_5, $\Delta L/L_{300\,K} = (L - L_{300\,K})/L_{300\,K}$, expressed as a percent is shown

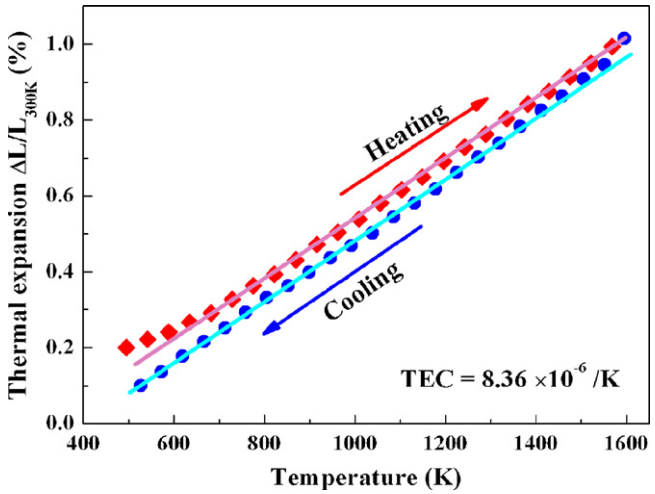

Fig. 2. Linear thermal expansion of polycrystalline Y_2SiO_5 bulk material.

in Fig. 2. The linear thermal expansion coefficient was determined in terms of the slope of thermal expansion vs. temperature during heating and cooling, and the linear CTE for γ-$Y_2Si_2O_7$ is $(8.36 \pm 0.5) \times 10^{-6}\,K^{-1}$. This value is lower than that obtained from the high-temperature power XRD measurement (Nowok et al.[18]) but slightly higher than those measured on the polycrystalline samples containing impurities like $Y_2Si_2O_7$ or $Y_{4.67}(SiO_4)_3O$ which has low TEC value (Table 1). Moreover, no abnormal expansion was observed in Fig. 2 in the examined temperature range, though a phase transformation from the low-temperature polymorph X1-Y_2SiO_5 to the high-temperature X2-Y_2SiO_5 around 1173 K was reported in some literatures.[18,19]

Fig. 3 is the thermal diffusivity data fitted by the second order polynomial equation, and the obtained result takes on a form like:

$$D_{th} = 0.01124 - 1.314 \times 10^{-5}T + 6.331 \times 10^{-9}T^2 \quad (3)$$

with a reliability value of $R^2 = 0.998$.

The temperature dependence of the heat capacity of Y_2SiO_5 is plotted in Fig. 4, in which the data from Y_2O_3 and SiO_2 are also given for comparison. Curve fitting of the experimental data

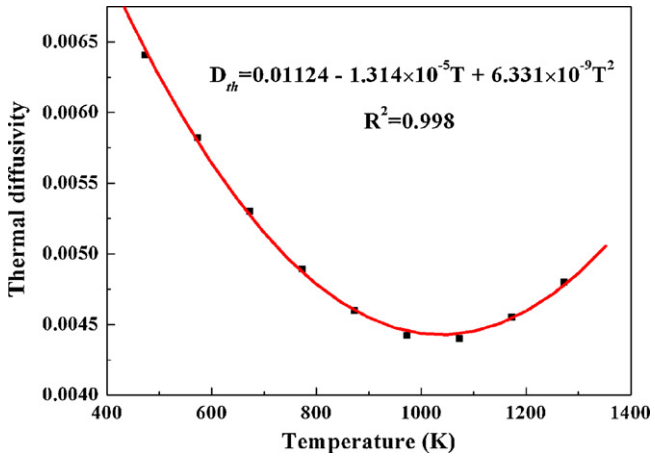

Fig. 3. Thermal diffusivity versus temperature for Y_2SiO_5.

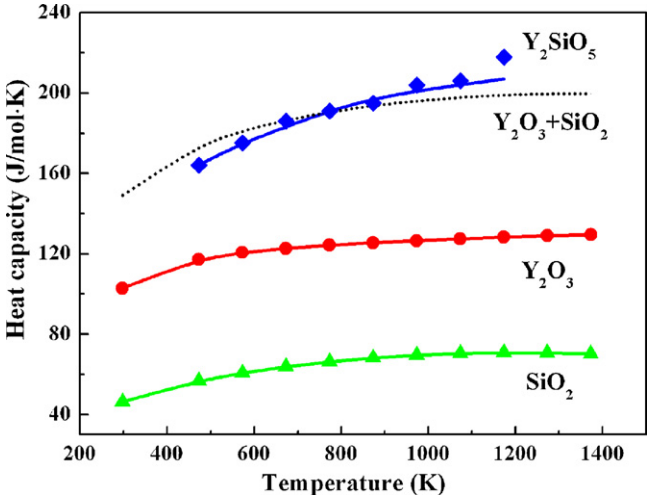

Fig. 4. Heat capacity versus temperature for Y_2SiO_5.

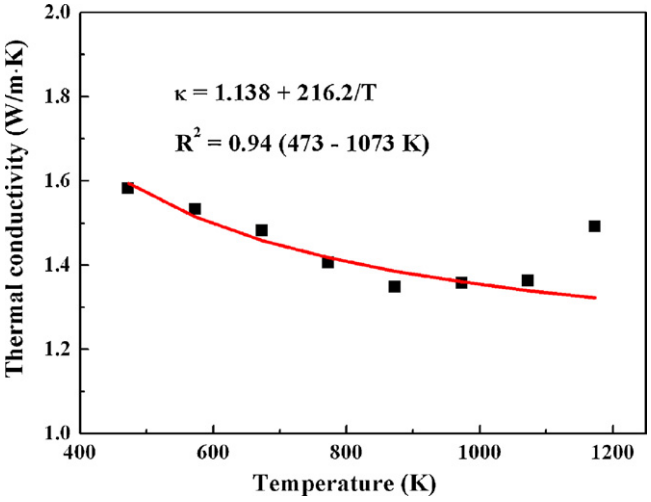

Fig. 5. Thermal conductivity versus temperature for Y_2SiO_5.

of Y_2SiO_5 yields:

$$C_p = 177.48 + 29.68 \times 10^{-3}T - 59.2 \times 10^5 T^{-2} \quad (4)$$

with a R^2 value of 0.994. The molar heat capacities extrapolated from this relationship are 120 and 215 J/(mol K) at room temperature (300 K) and high temperature (1400 K), respectively. The obtained heat capacity data of Y_2SiO_5 coincides will with the summation of $Y_2O_3 + SiO_2$[29] except for a minor deviation at the low and high limiting temperatures. Based on the Neumann–Kopp law, the heat capacity of Y_2SiO_5 can be determined as a summation of the atomic heat capacities of the constituent elements.[30] At temperatures above the Debye temperature (the Debye temperature for Y_2SiO_5 is 580 K, the calculation will be mentioned in later section), the molar heat capacity at constant volume, C_v, of each atom is about 3R (≈25 J/(mol K)) as predicted by the Dulong–Petit equation, where R is the gas constant.[31] Here, the calculated temperature-independent heat capacity of Y_2SiO_5 above Debye temperature is approximately 200 J/(mol K), which is slightly lower than the measured value at high temperatures (215 J/(mol K)) without taking into account of the difference between C_p and C_v (at room temperature, $(C_p - C_v)$ for a typical solid is about 1–8 J/(mol K) and it reaches a maximum at the melting point with a value of about 10% of C_v).[30]

The thermal conductivity of Y_2SiO_5 is plotted in Fig. 5. An inverse proportional fitting of the data yields the following relationship:

$$\kappa = 1.138 + \frac{216.2}{T} \quad (5)$$

From this equation, the thermal conductivities of Y_2SiO_5 are almost inverse proportional to temperature and are extrapolated to be 1.86 and 1.29 W/m K, respectively, at 300 K and 1400 K. As the microstructure and XRD of Y_2SiO_5 presented in Fig. 1, only a few residual small pores were observed at the grain boundaries and no grain-boundary phase was detected either by SEM or by XRD. The quantity of grain-boundary pores is too small to influence the thermal conductivity, and thus the measured thermal conductivity should be the intrinsic value of Y_2SiO_5. Therefore, Y_2SiO_5 has a thermal conductivity much lower than most commonly used thermal barrier coating materials, such as YSZ, $La_2Zr_2O_7$, etc.[32,33] Fig. 6 exhibits the thermal conductivities of some selected TBC materials as a function of temperatures.[5,32–34] Though a dense Y_2SiO_5 material was used for thermal conductivity measurement, its conductivity is only slightly higher than those of APS 7YSZ (air plasma sprayed 7 mol.% yttria stabilized zicornia) coating and monoclinic zirconia.[32]

3.2. Minimum high-temperature thermal conductivity

The thermal conductivity of a material describes the diffusivity of heat flow by phonon transport on temperature gradient. In the first successful model for thermal conductivity, Debye used an analogy of the kinetic theory of gases to derive an expression of the thermal conductivity as[35]:

$$\kappa = \frac{C_v \upsilon_m \Lambda}{3} \quad (6)$$

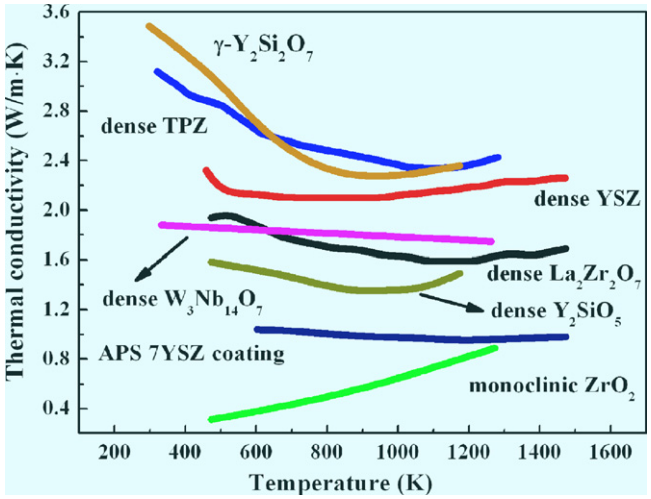

Fig. 6. Thermal conductivity of some selected thermal barrier coating candidates.

where C_v is the specific heat, υ_m the speed of sound and Λ the phonon mean free path. In the subsequent developments, a temperature that is characteristic of the material and now known as the Debye temperature, θ_D, plays a central role in phonon theories of thermal conductivity of solids. At the Debye temperature, the shortest wavelength of phonon corresponds to the size of the unit cell for simple cubic crystals.[35]

At a temperature above the Debye temperature, the heat capacity and the wave velocity are both approximate constant, whilst the mean free path for crystalline dielectric materials is nearly proportional to $1/T$.[36] In this case, the thermal conductivities of Y_2SiO_5 can be fitted perfectly by a $1/T$ equation in the range over 300–973 K. For the temperature above 973 K, the thermal conductivity should be a plateau and become independent of temperature. However, the actual condition is that the thermal conductivity reached a higher value 1.50 W/m K after a small platform in 873–1073 K. The abnormal increasing of thermal conductivity at temperatures higher than 1073 K may be resulted by the non-blocked radioactive heat transport through a material during measurement.[37] The measured minimum thermal conductivity value is 1.34 W/m K and this value sustained in a temperature range from 873 to 1073 K.

For most materials, such a minimum plateau value of thermal conductivity should be the minimum thermal conductivity κ_{min}. In selecting candidate materials for coating, it is necessary to know what the plateau value is and what temperature the transition from the $1/T$-dependance to plateau behavior occurs.[37] But experimentally the actual κ_{min} is very sensitive to the concentration of defects and preparation procedures, which make the comparison of thermal conductivity and the selection of material become difficult. Here, a calculated minimum thermal conductivity was used as a standard to choose suitable material for ETBC application.[5,37]

The Debye temperature, θ_D, of a solid is always associated with its melting point and can be calculated from the average sound velocity, υ_m[35]:

$$\theta_D = \frac{h}{k_B}\left[\frac{3n}{4\pi}\left(\frac{N_A d}{M}\right)\right]^{1/3}\upsilon_m \quad (7)$$

The average sound velocity is defined as[37]:

$$\upsilon_m = A\sqrt{\frac{E}{d}} \quad (8)$$

where M is the molecular mass, n the number of atoms in molecular, d the theoretic density, and E is Young's Modulus. A has a value of 0.87 ± 0.02. At the Debye temperature, the shortest wavelength of phonon is corresponding to the size of the primitive cell, a_0.

$$\theta_D = \frac{2\upsilon_m}{a_0 k_B} \quad (9)$$

The Debye temperature of Y_2SiO_5 can be calculated by Eqs. (7) and (8), and the value is 580 K. At the temperature higher than θ_D, the thermal conductivity approaches a minimum which is given by:

$$\kappa \rightarrow k_B \upsilon_m \Lambda \rightarrow k_B \upsilon_m \Lambda_{min} \quad (10)$$

Table 2
Calculated minimum thermal conductivity (W/m K) of Y_2SiO_5 and some selected ceramics[5,32–34,3,7]

Compound	k_{min}	Compound	k_{min}	Compound	k_{min}
SiC	3.00	$MgAl_2O_4$	2.34	γ-$Y_2Si_2O_7$	1.35
Al_2O_3	2.89	Mg_2SiO_4	2.00	$La_2Zr_2O_7$	1.20
MgO	2.56	Mullite	1.68	$LaPO_4$	1.13
TiO_2	2.07	$LaMgAl_{11}O_{19}$	1.48	Y_2SiO_5	1.13

where Λ_{min} is the minimum free path, which equals to the average atomic spacing. Ignoring the fact that the material of interest contain more than one type of atom per unit cell or per formula unit, an equivalent atom having a mean atomic mass given by M/n, where M is the molecular mass and n is the number of atoms per molecular, was employed to replace the different atoms in a molecule.[37]

Combining Eqs. (7)–(10), the minimum thermal conductivity can be expressed as[5,37]:

$$\kappa_{min} \rightarrow 0.87 k_B N_A^{2/3} \frac{n^{1/3} E^{1/2}}{M^{1/3} d^{1/6}} \quad (11)$$

The calculated minimum thermal conductivities of silicon carbide and selected EBC/TBC candidates are listed in Table 2,[5,32–34,37] wherein Y_2SiO_5 shows a low value of 1.13 W/m K, being close to the measured minimum value of 1.34 W/m K.

3.3. Potential coating applications for Y_2SiO_5

The low thermal conductivity of Y_2SiO_5 makes it very competitive as EBC/TBC candidates, especially when considering the match of thermal expansion coefficients between coating and substrate. At present, nickel-based superalloy is the most commonly used substrate material for gas turbine engines. Materials for the TBC layer are desired to have a thermal expansion coefficient close to that of nickel-based superalloys and have the lowest possible k value.

Fig. 7 presents the thermal expansion coefficient as a function of thermal conductivity for some coating materials and

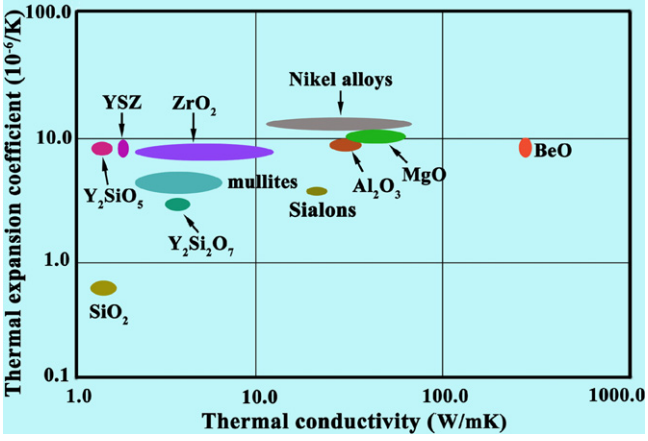

Fig. 7. Thermal expansion coefficient versus thermal conductivity for some promising thermal barrier coating materials on nickel-based superalloys.

Table 3
Linear thermal expansion coefficients of γ-$Y_2Si_2O_7$, Y_2SiO_5 and some non-oxide ceramics[5,32,39–41]

Compound	CTE	Compound	CTE	Compound	CTE
CrN	2.3	β-SiC	5.1	TiC	8.3
Si_3N_4	3.7	B_4C	5.5	**Y_2SiO_5**	**8.36**
γ-$Y_2Si_2O_7$	**3.90**	ZrC	6.6	Mo_2C	8.6
α-SiC	4.7	$Zr_3Al_3C_5$	7.7	Ti_3SiC_2	8.6
WC	4.9	$MoSi_2$	8.2	Ti_3AlC_2	9.0

nickel-based superalloys.[32,38] The nickel-based alloys used for turbine blades have a TEC from 14.0 to $16.0 \times 10^{-6}\,K^{-1}$ In Fig. 7, YSZ has a TEC of $\sim 9.0 \times 10^{-6}\,K^{-1}$ and Y_2SiO_5 of $\sim 8.4 \times 10^{-6}\,K^{-1}$. A very similar thermal expansion coefficient is notified between Y_2SiO_5 and nickel-based superalloy, guaranteeing a low thermal stress at the coating and substrate interfaces and thereby a good thermal cycling resistance. According to Fig. 7, Y_2SiO_5 can be regarded as the most suitable coating material for nickel-based superalloys if only considering the thermal expansion and thermal conductivity. Moreover, combining the low thermal conductivity, thermal expansion coefficient and good corrosion resistance, Y_2SiO_5 is also an excellent environmental barrier coating on YSZ TBC layer. As a source of Y^{3+}, Y_2SiO_5 EBC can prolong the lifetime of zirconia-based TBC by holding back the degradation aroused by the loss of Y stabilizer. Besides nickel-based superalloy, a lot of non-oxide ceramics with potential high-temperature structural applications are encumbered by the shortcomings of poor-oxidation resistance, inferior environmental durability and so on. It is clear that $Y_2Si_2O_7$ has a very similar thermal expansion coefficient with that of silicon carbide or nitride ceramics and $Y_2Si_2O_7$ is also a candidate for EBC or oxygen-resistant coating on these ceramics.[34] As shown in Table 3, Y_2SiO_5 in combination with γ-$Y_2Si_2O_7$ can provide a good protection to the non-oxide ceramics in oxidizing or combusting environment, though the thermal expansion coefficients of these non-oxide ceramics varies in a wide range.[5,32,39–41] Therefore, ceramics in Y–Si–O system are promising coating materials due to their unique thermal properties and superior environmental durability.

4. Conclusion

In summary, the thermal properties of Y_2SiO_5 were systematically studied, including thermal expansion, thermal diffusivity, heat capacity and thermal conductivity. The linear thermal expansion coefficient of the single-phase polycrystalline bulk Y_2SiO_5 material determined by the push-rod dilatometer is $(8.36 \pm 0.5) \times 10^{-6}\,K^{-1}$ in the temperature range from 300 to 1573 K. During the test, no polymorph transformation was detected either in the heating or the cooling process.

The measured minimum thermal conductivity of Y_2SiO_5 is 1.34 W/m K at 873 K to 1173 K, which is lower than most commonly used thermal barrier coating material such as YSZ. The low thermal conductivity, low oxygen permeability as well as a relatively high thermal expansion coefficient ensure Y_2SiO_5 being a very competitive candidate material for both environmental/thermal barrier and oxygen-resistant coatings, especially in combination with $Y_2Si_2O_7$ sometimes.

Acknowledgements

This work was supported by the National Outstanding Young Scientist Foundation for Y.C. Zhou under Grant No. 59925208, Natural Sciences Foundation of China under Grant Nos. 50232040, 50302011, 90403027, 50772114.

References

1. Ziegler, G., Neinrich, J. and Wötting, G., Review, relationships between processing, microstructure and properties of dense and reaction-bonded silicon nitride. *J. Mater. Sci.*, 1987, **22**, 3041–3086.
2. Jacobson, N. S., Corrosion of Silicon-based ceramics in combustion environments. *J. Am. Ceram. Soc.*, 1993, **76**, 3–28.
3. Jacobson, N. S., Kinetics and mechanism of corrosion SiC by molten salts. *J. Am. Ceram. Soc.*, 1986, **69**, 74–82.
4. Lee, K. N., Fox, D. S. and Bansal, N. P., Rare earth silicate environmental barrier coatings for SiC/SiC composites and Si_3N_4 ceramics. *J. Eur. Ceram. Soc.*, 2005, **25**, 1705–1715.
5. Clarke, D. R. and Phillpot, S. R., Thermal barrier coating materials. *Mater. Today*, 2005, **8**, 22–29.
6. Ueno, S., Jayaseelan, D. D. and Ohji, T., Development of oxide-based EBC for silicon nitride. *Inter. J. Appl. Ceram. Technol.*, 2004, **1**, 362–373.
7. Warshaw, J. and Roy, R., Crystal chemistry of rare earth sesquioxides, aluminates and silicates. *Prog. Sci. Technol., Rare Earths*, 1963, **1**, 203–221.
8. Shin, S. H., Jeon, D. Y. and Suh, K. S., Emission band shift of the cathodoluminescence of Y_2SiO_5:Ce phosphor affected by its concentration. *Jpn. J. Appl. Phys., Part 1*, 2001, **40**, 4715–4719.
9. Bottger, T., Sun, Y., Reinemer, G. J. and Core, R. L., Diode laser frequency stabilization to transient spectral holes and spectral diffusion in Er^{3+}:Y_2SiO_5 at 1536 nm. *J. Lumin.*, 2001, **94/95**, 565–568.
10. Deka, C., Chai, B., Shimony, Y., Zhang, X., Munin, E. and Bass, M., Laser performance of Cr^{4+}–Y_2SiO_5. *Appl. Phys. Lett.*, 1992, **61**, 2141–2143.
11. Lange, F. F., Singhal, S. C. and Kuznicki, R. C., Phase relations and stability studies in the Si_3N_4–SiO_2–Y_2O_3 pseudoternary system. *J. Am. Ceram. Soc.*, 1977, **60**, 249–252.
12. Gauckler, L. J., Hohnke, H. and Tien, T. Y., The system Si_3N_4–SiO_2–Y_2O_3. *J. Am. Ceram. Soc.*, 1980, **63**, 35–37.
13. Cinibulk, M. K. and Thomas, G., Grain-boundary-phase crystallization and strength of silicon nitride sintered with a YSiAlON glass. *J. Am. Ceram. Soc.*, 1990, **73**, 1606–1612.
14. Lichvár, P., Šajgalík, P., Liška, M. and Galusek, D., CaO–SiO_2–Al_2O_3–Y_2O_3 glass as model grain boundary phases for Si_3N_4 ceramics. *J. Eur. Ceram. Soc.*, 2007, **27**, 429–436.
15. Levin, E. M., Robbins, C. R. and McMurdie, H. F., *Phase Diagrams for Ceramists—1969 Supplement*. The American Ceramic Society Inc, Columbus, OH, 1969, p. 76 (Fig. 2388).
16. Ogura, Y., Kondo, M., Morimoto, T., Notomi, A. and Sekigawa, T., Oxygen permeability of Y_2SiO_5. *Mater. Trans.*, 2001, **42**, 1124–1130.
17. O'Bryan, H. M., Gallagher, P. K. and Berkstresser, G. W., Thermal expansion of Y_2SiO_5 single crystal. *J. Am. Ceram. Soc.*, 1988, **71**, C42–C43.
18. Nowok, J. W., Kay, J. P. and Kulas, R. J., Thermal expansion and high-temperature phase transformation of the yttrium silicate Y_2SiO_5. *J. Mater. Res.*, 2001, **16**, 2251–2255.
19. Fukuda, K. and Matsubara, H., Anisotropic thermal expansion in yttrium silicate. *J. Mater. Res.*, 2003, **18**, 1715–1722.
20. Ogura, Y., Kondo, M. and Morimoto, T., Y_2SiO_5 as oxidation resistance coating for C/C composites. In *Proceed. of the 10th Inter. Confer. on Comp. Mater. (ICCM-10), Vol. IV*, 1995, p. 767.
21. Apricio, M. and Duran, A., Yttrium silicate coatings for oxidation protection of carbon-silicon carbide composites. *J. Am. Ceram. Soc.*, 2000, **83**, 1351–1355.

22. Wagner, S., Seifert, H. J. and Aldinger, F., High-temperature reaction of C/C–SiC composites with ceramic coatings. In *Proceed. of the 10th Inter. Confer. on Advan. Mater. & Mater Proce. (ICAMMP-2002)*, 2002, p. 71.
23. Webster, J. D., Westwood, M. E., Hayes, F. H., Day, R. J., Taylor, R., Duran, A. *et al.*, Oxidation protection coatings for C/SiC based on yttrium silicate. *J. Eur. Ceram. Soc.*, 1998, **18**, 2345–2350.
24. Huang, J., Li, H., Zeng, X., Li, K., Xiong, X., Hunag, M. *et al.*, A new SiC/yttrium silicate/glass multi-layer oxidation protective coating for carbon/carbon composites. *Carbon*, 2004, **42**, 2329–2366.
25. Sun, Z. Q., Zhou, Y. C. and Li, M. S., Effect of $LiYO_2$ additive on synthesis and pressureless sintering of Y_2SiO_5. *J. Mater. Res.*, 2008, **23**, 732–736.
26. Sun, Z. Q., Wang, J. Y., Li, M. S. and Zhou, Y. C., Mechanical properties and damage tolerance of Y_2SiO_5. *J. Eur. Ceram. Soc.*, 2008, **28**, 2895–2901.
27. ASTM E 1461-01, Standard test method for thermal diffusivity by flash method.
28. Shinzato, K. and Baba, T., A laser flash apparatus for thermal diffusivity and specific heat capacity measurements. *J. Therm. Anal. Calcor.*, 2001, **64**, 413–422.
29. Brain, I., *Thermochemical Data of Pure Substances*. Wiley-VCH Verlag GmbH, Weinheim, Germany, 1995.
30. Gopal, E. S. R., *Specific Heats at Low Temperatures*. Plenum, New York, 1996.
31. Kittel, C., *Introduction to Solid State Physics* (*6th edition*). John Wiley & Sons Inc., New York, 1986.
32. NIST material properties database in web of the American Ceramics Society web site: http://www.ceramics.org/publications/ceramic_properties_databases.aspx.
33. Vassen, R., Cao, X., Tietz, F., Basu, D. and Stöver, D., Zirconates as new material for thermal barrier coating. *J. Am. Ceram. Soc.*, 2000, **83**, 2023–2028.
34. Sun, Z. Q., Zhou, Y. C., Wang, J. Y. and Li, M. S., Thermal properties and thermal shock resistance of γ-$Y_2Si_2O_7$. *J. Am. Ceram. Soc.*, 2008, **91**, 2623–2629.
35. Anderson, O. L., A simplified method for calculating the Debye temperature from elastic constants. *J. Phys. Chem. Solids*, 1963, **24**, 909–917.
36. Kingery, W. D., Thermal conductivity: XII, temperature dependence of conductivity for single-phase ceramics. *J. Am. Ceram. Soc.*, 1955, **38**, 251–255.
37. Clarke, D. R., Materials selection guidelines for low thermal conductivity thermal barrier coatings. *Surf. Coat. Tech.*, 2003, **163–164**, 67–74.
38. Hass, D.D., Direct vapor deposition of thermal barrier coatings. PhD. Dissertation. University of Virginia; 2000.
39. He, L. F., Wang, J. Y., Bao, Y. W. and Zhou, Y. C., Elastic and thermal properties of $Zr_2Al_3C_4$: experimental investigations and *ab initio* calculations. *J. Appl. Phys.*, 2007, **102**, 043531.
40. Barsoum, M. W., El-Raghy, T., Rawn, C. J., Porter, W. D., Wang, H., Payzant, E. A. *et al.*, Thermal properties of T_3SiC_2. *J. Phys. Chem. Solids*, 1999, **60**, 429–439.
41. Tzenov, N. V. and Barsoum, M. W., Synthesis and characterization of Ti_3AlC_2. *J. Am. Ceram. Soc.*, 2000, **83**, 825–832.